Anomalous Faraday effect in a $\mathcal{PT}$-symmetric dielectric slab

Vladimir Gasparian [a], Peng Guo [a,*], Esther Jódar [b]

[a] *Department of Physics and Engineering, California State University, Bakersfield, CA 93311, USA*
[b] *Departamento de Física Aplicada, Universidad Politécnica de Cartagena, E-30202 Murcia, Spain*

A R T I C L E   I N F O

A B S T R A C T

In this letter we discuss a phase transition-like anomalous behavior of Faraday rotation angles in a simple parity-time ($\mathcal{PT}$) symmetric model with two complex δ-potential placed at both boundaries of a regular dielectric slab. In anomalous phase, the value of one of Faraday rotation angles turns negative, and both angles suffer spectral singularities and yield strong enhancement near singularities.

© 2022 The Authors. Published by Elsevier B.V. This is an open access article under the CC BY-NC-ND license (http://creativecommons.org/licenses/by-nc-nd/4.0/).

1. Introduction

Faraday rotation (FR) is a magneto-optical phenomenon that rotates the polarization of light. It occurs either due to the internal property of the medium or to the external magnetic field applied. In both cases, the dielectric permittivity tensor of the system becomes anisotropic [1]. The Faraday effect shows a wide range of applications in various fields of modern physics, such as, (i) measuring magnetic field in astronomy [2]; (ii) construction of optical isolators for fiber-optic telecommunication systems [3]; or (iii) optical circulators that are used in the design of microwave integrated circuits [4–6]. Usually it is necessary either a large size or a strong external magnetic field in order to obtain a large FR in bulk magneto-optical materials. [7,8]. However, for small size systems, where the de Broglie wavelength is compatible with size of systems, a large enhancement of the FR and as well as a change in the sign of the FR can be obtained by incorporating several nanoparticles and their composites in nanomaterials, see e.g. Refs. [9–11]. The aim of this letter is to exhibit that the large enhancement of Faraday rotation and the anomalous phase transition-like effect may occur when the medium is parity-time ($\mathcal{PT}$) symmetric. Moreover, in certain range of model parameters of a $\mathcal{PT}$-symmetric system a *non-trivial* transition occurs with a change of sign of FR. *Non-triviality* of the transition of FR only happens in a few well-known cases, such as (1) when the sign of the constant Verdet is changed or when either the magnetic field or the direction of the light is reversed; (2) in a new type artificial left handed materials (metamaterials) with negative permittivity ϵ and permeability μ, as shown in Refs. [12–16], the sign of FR is negative because the refractive index n becomes negative. It should be noted that in metamaterials FR changes the sign only in a narrow frequency range, while in the $\mathcal{PT}$ system discussed here, the change occurs in a fairly large frequency range.

In recent years, numerous remarkable novel phenomena have been discovered within $\mathcal{PT}$ symmetric systems [17–24], including real spectra of non-Hermitian operators [17,18,25,26], spectral singularities [27–29], the violation of the normal conservation of the photon flux that leads to anisotropic transmission resonances [30], etc. Most importantly, $\mathcal{PT}$ symmetric systems have been experimentally developed in optics [22–24], atomic gases [31,32], plasmonic waveguides [33,34] or acoustic [35].

In this letter, we illustrate that the Faraday rotation angles of the polarized light traveling through a $\mathcal{PT}$-symmetric material displays phase transition-like anomalous behaviors. With a simple $\mathcal{PT}$-symmetric dielectric slab model, we show that in one phase (normal phase), the angle of Faraday rotation behaves normally as in regular dielectric slab with a positive permittivity, and stay positive all the time as expected. In the second anomalous phase, the angle of Faraday rotation may change the sign and turn into negative. Two phases are separated by the parameters of $\mathcal{PT}$-symmetric model. In addition, the spectral singularities occur in the second anomalous phase. The Faraday rotation angles thus yield a strong enhancement near spectral singularities. In this sense, $\mathcal{PT}$-systems seem to be a good candidate for constructing fast tunable and switchable polarization rotational ultrathin magneto-optical devices in a wide frequency range with a giant Faraday rotation.

* Corresponding author.
E-mail addresses: vgasparyan@csub.edu (V. Gasparian), pguo@csub.edu (P. Guo), esther.jferrandez@upct.es (E. Jódar).
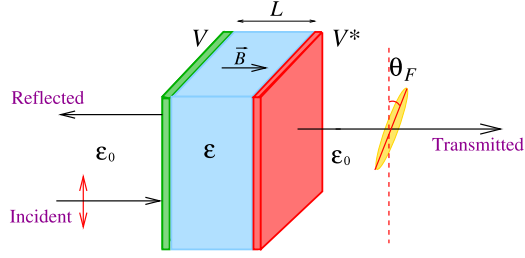
Fig. 1. Demo plot of a $\mathcal{PT}$-symmetric dielectric slab model with two balanced complex narrow slabs placed at both ends of a real dielectric slab.

2. The theory of Faraday effect in a $\mathcal{PT}$-symmetric dielectric slab

Let us consider a $\mathcal{PT}$-symmetric dielectric slab with a finite spatial extent of length L along x direction, where the permittivity of the slab has balanced gain and loss,

$$\epsilon\left(x - \frac{L}{2}\right) = \epsilon^*\left(-x + \frac{L}{2}\right). \tag{1}$$

A linearly polarized electromagnetic plane wave with angular frequency ω enters the slab from the left at normal incidence propagating along the x direction. The polarization direction of electric field of incident wave is taken as the z-axis: $\boldsymbol{E}_0(x) = e^{ik_0 x}\hat{z}$, where $k_0 = \frac{\omega}{c}\sqrt{\epsilon_0}$ stands for the wave vector and ϵ_0 denotes the dielectric constant of vacuum. A weak magnetic field $\boldsymbol{B}$, which preserves the linearity of Maxwell's equations, is applied in the x-direction and is confined into the slab, see Fig. 1. The scattering of incident wave by the dielectric slab is described by Schrödinger-like equations, see e.g. Refs. [36,37],

$$\left[\frac{d^2}{dx^2} + \frac{\omega^2 \epsilon_{\pm}(x)}{c^2}\right] E_{\pm}(x) = 0, \tag{2}$$

where $E_{\pm} = E_y \pm iE_z$ are circularly polarized electric fields. The $\epsilon_{\pm}(x)$ is defined by, see e.g. Refs. [36,37],

$$\epsilon_{\pm}(x) = \begin{cases} \epsilon(x) \pm g, & x \in [0, L], \\ \epsilon_0, & \text{otherwise,} \end{cases} \tag{3}$$

where g is the gyrotropic vector along the magnetic-field direction. The external magnetic field $\boldsymbol{B}$ is included into the gyrotropic vector g to make the calculations valid for the cases of both external magnetic fields and magneto-optic materials. The magnetic field causes the direction of linear polarization to rotate while light propagates through the medium. As a consequence, the electromagnetic wave is elliptically polarized and the major axis of the ellipse is rotated with respect to the original direction of polarization. The angle of Faraday rotation, θ_1, and the degree of ellipticity, θ_2, are defined by [36,37]

$$\theta_1 = \frac{\psi_+ - \psi_-}{2}, \quad \theta_2 = \frac{1}{4}\ln\frac{T_+}{T_-}, \tag{4}$$

where $T_{\pm}$ and $\psi_{\pm}$ are the transmission coefficients and phase of transmission amplitudes, $t_{\pm} = \sqrt{T_{\pm}}e^{i\psi_{\pm}}$, of transmitted electric fields:

$$E_{\pm}(x > L) = \pm it_{\pm}e^{ik_0 x}. \tag{5}$$

For the dielectric material with real value of permittivity, the scattering S-matrix can be parameterized by two independent real scattering phaseshifts, $\delta_{\pm}^{(1/2)}$. The transmission coefficients and phases $\psi_{\pm}$ are given in terms of scattering phaseshifts by

$$\sqrt{T_{\pm}} = \cos(\delta_{\pm}^{(1)} - \delta_{\pm}^{(2)}), \quad \psi_{\pm} = \delta_{\pm}^{(1)} + \delta_{\pm}^{(2)}. \tag{6}$$

Hence both angles θ_1 and θ_2 are real and well defined. As discussed in Ref. [38], for the scattering with a complex potential in general, scattering phaseshifts become complex. Therefore, with a complex dielectric slab, both θ_1 and θ_2 are complex in general, and physical meaning of both angles become ambiguous.

In a $\mathcal{PT}$-symmetric system, the parameterization of scattering S-matrix now requires three independent real functions: two phaseshifts and one inelasticity, $\eta_{\pm} \in [1, \infty]$, see Ref. [38]. The phases of a $\mathcal{PT}$-symmetric system, $\psi_{\pm}^{(\mathcal{PT})}$, are still given by the sum of two real phaseshifts as in Eq. (6), thus it remains real. The transmission coefficients of $\mathcal{PT}$-symmetric system also remain real but now depend on inelasticity as well,

$$\sqrt{T_{\pm}^{(\mathcal{PT})}} = \eta_{\pm}\cos(\delta_{\pm}^{(1)} - \delta_{\pm}^{(2)}). \tag{7}$$

Therefore, with balanced gain and loss, the reality of both Faraday rotation angles θ_1 and θ_2 is warranted in a $\mathcal{PT}$-symmetric system. In Ref. [38], it is also shown that the generalized Friedel formula relates the derivative of sum of two phaseshifts, $\frac{d}{d\omega}(\delta_{\pm}^{(1)} + \delta_{\pm}^{(2)}) = \frac{d\psi_{\pm}^{(\mathcal{PT})}}{d\omega}$, to the integrated generalized density of states of the $\mathcal{PT}$-symmetric system, which turns out to be real for a $\mathcal{PT}$-symmetric system. Hence the reality of FR angles in a $\mathcal{PT}$-symmetric system can also be understood based on the generalized Friedel formula. However, the positivity of generalized density of state in $\mathcal{PT}$-symmetric systems is no longer guaranteed. Therefore the FR angles of $\mathcal{PT}$-symmetric systems show an anomalous behavior becoming negative.

3. A simple $\mathcal{PT}$-symmetric model

We use in our calculations a very simple $\mathcal{PT}$-symmetric model to illustrate the anomalous behavior of FR angles by putting two complex delta potentials at both ends of the dielectric slab with a positive and real permittivity ($\epsilon > 0$ and real),

$$\epsilon(x) = \epsilon + V\delta(x) + V^*\delta(x - L), \quad V = V_1 + iV_2 = |V|e^{i\varphi_V}. \tag{8}$$

We adopt this model because it lets us obtain quite easily the analytical expressions, and some techniques and conclusions that were developed in Refs. [36,37] can be applied directly in this work. The $\mathcal{PT}$-symmetric double complex boundaries model is similar to the model by considering $\mathcal{PT}$-symmetric complex dielectric permittivities of slab: $\epsilon(x \in [0, \frac{L}{2}]) = \epsilon$ for first half of slab and $\epsilon(x \in [\frac{L}{2}, L]) = \epsilon^*$ for another half. Both models can be solved relatively easily and analytically, and both show similar anomalous behaviors of FR angles. No significant difference between two models has been observed. The basis and physical reason for this conclusion is that the two-boundary model discussed in the manuscript can be considered as having two slabs with changeable thickness and potential force, so the delta potentials are the limit of the two finite potentials of a square. Hence we will simply present some results of double complex boundaries model, and it is sufficient to show anomalous behavior of Faraday rotation angles in $\mathcal{PT}$-symmetric systems.

For weak magnetic field ($g \ll 1$) and constant dielectric permittivity in the slab, the Faraday rotation angles in Eq. (4) can be evaluated in terms of perturbation expansion of the weak magnetic field. The leading order expressions are obtained in Refs. [36,37] and are given by

$$\theta_1 = \frac{g}{2n}\frac{\partial\psi}{\partial n}, \quad \theta_2 = \frac{g}{4n}\frac{\partial\ln T}{\partial n}, \tag{9}$$

where $n = \sqrt{\epsilon}$ is the refractive index of the slab. The T and ψ stand for the coefficient of transmission and the phase in the absence of the external magnetic field $\boldsymbol{B}$. The conclusion in Eq. (9)

also apply to double complex boundaries $\mathcal{PT}$ model in Eq. (8). For the simple double complex boundaries $\mathcal{PT}$-symmetric model, the transmission amplitude, $t = \sqrt{T}e^{i\psi}$, can be easily obtained by matching boundary conditions method. Hence we find

$$t(\omega) = \frac{e^{-ik_0 L}\csc(kL)}{R(\omega) - iI(\omega)}, \qquad (10)$$

where

$$R(\omega) = \cot(kL) - Z\frac{\omega V_1}{cn_0},$$

$$I(\omega) = \frac{\omega V_1}{cn_0}\cot(kL) + \frac{1 + Z^2\left(1 - (\frac{\omega|V|}{cn_0})^2\right)}{2Z}. \qquad (11)$$

$Z = \sqrt{\frac{\epsilon_0}{\epsilon}} = \frac{n_0}{n}$ is the "relative" impedance of the dielectric slab, and $k = \frac{\omega}{c}n$ denotes the wave vector of propagating waves inside the dielectric slab. The transmission amplitude t can also be obtained by the Green's function approach [39]. We remark that the Green's function approach is a better tool for more sophisticated multilayer systems, which is based on the exact calculation of the Green's function (GF) of a photon for a given dielectric permittivity profile $\epsilon(x)$. The GF approach is compatible with the transfer matrix method and has been widely used to calculate the average density of states over a sample, the energy spectrum of elementary excitations [39], or the characteristic barrier tunneling time [40], among others. The coefficient of transmission T and the phase ψ are thus explicitly given by

$$T(\omega) = \frac{\csc^2(kL)}{R^2(\omega) + I^2(\omega)}, \quad \psi(\omega) = \tan^{-1}\left[\frac{I(\omega)}{R(\omega)}\right]. \qquad (12)$$

We remark that unphysical units are adopted in this work for a simple model: the length of slab L is used to sent up the physical scale, V and $\epsilon = n^2$ carry the dimensions of $1/L$ and $1/L^2$ respectively. The ω/c is hence a dimensionless quantity.

3.1. Spectral singularities

The resonance states with vanishing spectral width appear in non-Hermitian complex potential scattering theory and yield divergences of reflection and transmission coefficients of scattered states, which are usually referred as spectral singularities, see e.g. Refs. [27–29]. Therefore, near spectral singularities it should be expected a strong enhancement of both Faraday rotation angles. Specifically, for the double complex boundaries $\mathcal{PT}$-symmetric model considered in this letter, the spectral singularities occur when both conditions, $R(\omega) = 0$ and $I(\omega) = 0$, are satisfied. Hence the solutions of spectral singularities can be obtained by

$$\left(\frac{1 + \frac{1 + \cot^2(kL)}{Z^2}}{1 + \frac{1 + 2\cot^2(kL)}{Z^2}}, \frac{1 + \frac{1 + 2\cot^2(kL)}{Z^2}}{(\frac{\omega}{cn_0})^2}\right) = (\sin^2\varphi_V, |V|^2). \qquad (13)$$

Since the left-hand side of the first condition in Eq. (13) is confined to the range $[\frac{1}{2}, 1]$, the spectral singularities exist only when the phase angle φ_V is in the range $[\frac{\pi}{4}, \frac{\pi}{2}]$ or $[\frac{\pi}{2}, \frac{3\pi}{4}]$. Henceforth, all discussions will be for the range: $\varphi_V \in [0, \frac{\pi}{2}]$, which is sufficient due to the symmetry of our model.

The solutions of spectral singularities on real ω axis can be visualized graphically by observing the intersection of a curve and a line with (x, y) coordinates given by both sides of Eq. (13) for a fixed $|V|$, see Fig. 2 as a example. The curve that is plotted with coordinates given by left-hand side of Eq. (13) as function of ω is bound in the region with $x \in [\frac{1}{2}, 1]$. For a fixed $|V|$, the solutions of spectral singularities can only be found in a finite range:
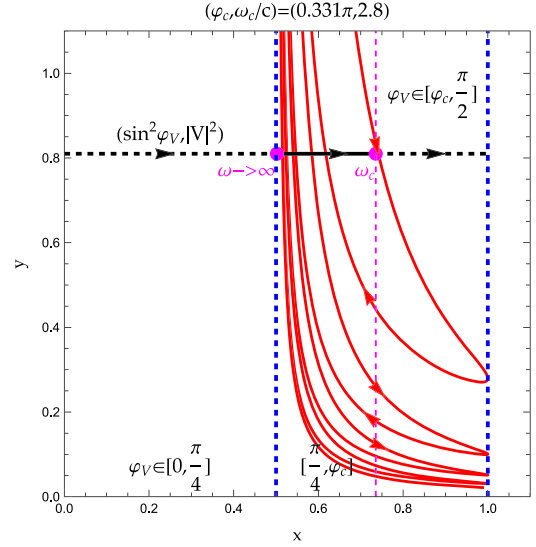

Fig. 2. Spectral singularities condition plot: the parametric plot of solid red curve is generated with (x, y) coordinates given by left-hand side of Eq. (13) as the function of $\omega/c \in [0, 10]$. The solid red curve is bound by two blue vertical lines located at $x = \frac{1}{2}$ and $x = 1$. The solid black line is generated with coordinates of $(\sin^2\varphi_V, |V|^2)$ by varying φ_V in the range of $[0, \frac{\pi}{4}]$ (dashed black), $[\frac{\pi}{4}, \varphi_c]$ (solid black) and $[\varphi_c, \frac{\pi}{2}]$ (dashed black). The arrows indicate increasing ω and φ_V directions. The value of ω of spectral singularities for fixed V is given by intersection of black line and red curve. The model parameters are chosen as: $|V| = 0.9$, $n_0 = 1$, $L = 1$ and $Z = 0.7$. (For interpretation of the colors in the figure(s), the reader is referred to the web version of this article.)

$\varphi_V \in [\frac{\pi}{4}, \varphi_c]$, where φ_c stands for upper bound of range, see e.g. Fig. 2. From Eq. (13), the spectral singularity solutions ω is related to φ_V by $\omega/c = \frac{n_0}{|V|Z}\frac{1}{\sqrt{|\cos(2\varphi_V)|}}$. Hence as φ_V approaches lower bound of range at $\frac{\pi}{4}$, the spectral singularity solution occurs at large frequency: $\omega \to \infty$. When φ_V is increased, the solution of spectral singularity moves toward lower frequencies. As φ_V approaches the upper bound of range at φ_c, the spectral singularity solution thus reaches its lowest value at ω_c, see e.g. Fig. 2.

3.2. Phase transition-like phenomenon of Faraday rotation angle θ_1

For a regular dielectric slab with positive and real permittivity ($\epsilon > 0$ and real), the Faraday rotation angle θ_1 must be also real and positive. However, in a $\mathcal{PT}$ system, the Faraday rotation angle θ_1 shows a phase transition-like anomalous behavior, and two phases are separated by model parameter φ_V:

(Phase I) for $\varphi_V \in [0, \frac{\pi}{4}]$, the value of θ_1 is always positive. No spectral singularities can be found and $\mathcal{PT}$-symmetric slab behaves just as a regular dielectric slab;

(Phase II) for $\varphi_V \in [\frac{\pi}{4}, \frac{\pi}{2}]$, the value of θ_1 may change the sign and turn negative. When $\varphi_V \in [\frac{\pi}{4}, \varphi_c]$, the spectral singularities occur and θ_1 starts showing negative values. The negative θ_1 only show up at large ω region when $\varphi_V \sim \frac{\pi}{4}$, and then gradually moves toward the lower frequency region as φ_V is increased. As φ_V continues increasing up to region of $[\varphi_c, \frac{\pi}{2}]$ that is also free of spectral singularities, the negativity of θ_1 persists, see e.g. Fig. 3.

Hence, a $\mathcal{PT}$ system yields a phase transition-like anomalous behavior of Faraday rotation angle θ_1, the $\varphi_V = \frac{\pi}{4}$ is the critical value that separates the positivity and negativity phases of θ_1.

The phase transition-like behavior of θ_1 can be understood intuitively by considering limiting case of $|V| \to \infty$,

$$\theta_1 \overset{|V| \to \infty}{\to} \cos(2\varphi_V)\frac{g}{2n}\left(\frac{\omega|V|}{cn_0}\right)^2\frac{ZT(\omega)}{2n}\left(kL - \frac{\sin(2kL)}{2}\right). \qquad (14)$$

Now, we can see very clearly that the sign of θ_1 is totally determined by φ_V in this limiting case.
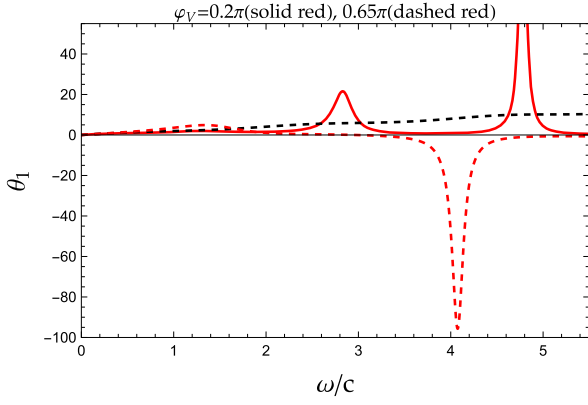
Fig. 3. Comparison of θ_1 of $\mathcal{PT}$-symmetric model with various values of φ_V: $\varphi_V = 0.2\pi$ (solid red) and 0.65π (dashed red). The regular θ_1 angle (dashed black curve) with no complex boundaries by setting $V = 0$ is also plotted. The parameters are taken as: $|V| = 0.9$, $n_0 = 1$, $L = 1$, and $Z = 0.7$.
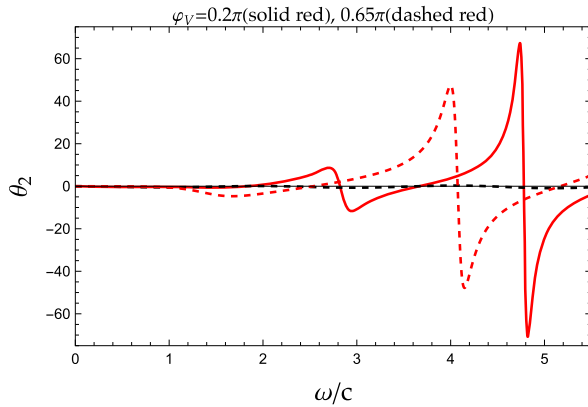

Fig. 4. Comparison of θ_2 of $\mathcal{PT}$-symmetric model with various values of φ_V: $\varphi_V = 0.2\pi$ (solid red) and 0.65π (dashed red). The regular θ_2 angle (dashed black curve) with no complex boundaries by setting $V = 0$ is also plotted. The parameters are taken as: $|V| = 0.9$, $n_0 = 1$, $L = 1$, and $Z = 0.7$.

The anomalous negativity behavior of θ_1 can also be illustrated analytically at another limiting case by setting $V_1 = 0$ and $\varphi_V = \frac{\pi}{2}$,

$$\theta_1 \stackrel{V_1 \to 0}{\to} \frac{gT(\omega)}{2n} \frac{\frac{2kL+\sin(2kL)}{2} + Z^2 \frac{2kL-\sin(2kL)}{2}[1 - (\frac{\omega V_2}{cn_0})^2]}{2n_0}. \quad (15)$$

Both $2kL \pm \sin(2kL)$ are positive definite functions, hence as $\frac{\omega V_2}{cn_0} > 1$, the sign of FR angle θ_1 changes from positive to negative.

4. Discussion and summary

In summary, using a simple $\mathcal{PT}$-symmetric model with two complex δ-potential placed at both boundaries of a regular dielectric slab, we show that FR angles display a phase transition-like anomalous behavior. In regular phase, Faraday rotation angles behave as normal as in a regular dielectric slab. In anomalous phase, FR angle θ_1 turns negative, and both angles θ_1 and θ_2 suffer spectral singularities and yield strong enhancement near singularities (see Fig. 4). The critical value of phase transition is controlled by the parameter of $\mathcal{PT}$-symmetric model. A very similar anomalous phase transition-like behavior to FR is expected in reflected light (Kerr effect, see e.g. Ref. [37]).

On the contrary to phase transition-like anomalous θ_1 behavior during transition, angle θ_2 doesn't exhibit the significant change of nature except that it also suffers the spectral singularities in
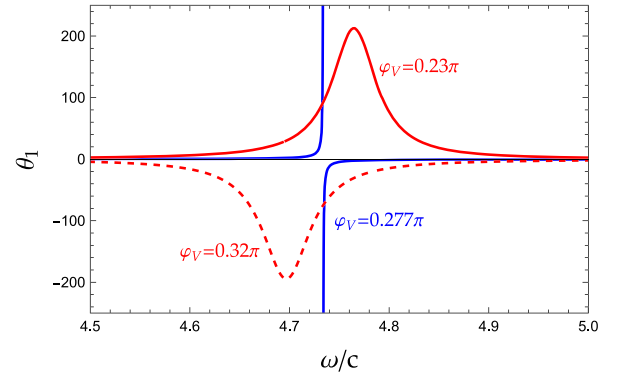

Fig. 5. Behavior of θ_1 of $\mathcal{PT}$-symmetric model as φ_V is increased across spectral singularities that is located at $(\omega/c, \varphi_V) = (4.73, 0.277\pi)$: $\varphi_V = 0.23\pi$ (solid red), $\varphi_V = 0.277\pi$ (solid blue) and $\varphi_V = 0.32\pi$ (dashed red). The parameters are taken as: $|V| = 0.9$, $n_0 = 1$, $L = 1$, and $Z = 0.7$.

anomalous phase. This can be understood from the definition of θ_2 in Eq. (4) and the expression of transmission coefficients in Eq. (7). The angle θ_2 is an oscillating function regardless that dielectric slab is regular or $\mathcal{PT}$-symmetric. In $\mathcal{PT}$ systems, the conservation law of scattering must be generalized, see e.g. Ref. [41], the transmission coefficients are no longer bound in range of $[0, 1]$ due to the inelasticity functions of $\mathcal{PT}$ systems $\eta_\pm \in [1, \infty]$. However, because angle θ_2 depends only on the ratio of $T_\pm$, the oscillating nature of θ_2 remains unchanged even in $\mathcal{PT}$ systems with unbound $T_\pm$. In addition, in both phases, we observe that θ_2 vanish near frequencies of resonant peaks appeared in θ_1. The vanishing θ_2 angle represents the purely linearly polarized wave with no ellipticity. The angle θ_2 also displays the sawtooth behavior: the amplitude of angle θ_2 keep growing as frequency is increased, and it is periodically repeated and changed sharply both in magnitude and in sign near the resonance frequencies.

As suggested in Ref. [42], the phase transition-like behavior of θ_1 is closely related to the motion of the pole of transition amplitudes. Near the pole, the transmission amplitude is approximated by

$$t(\omega) \propto \frac{1}{\omega - \omega_{pole}}, \quad (16)$$

where $\omega_{pole} = \omega_{Re} + i\omega_{Im}$ is the pole position in complex k-plane, see Eq. (24) in [42]. The phase of transmission amplitude is dominated by

$$\frac{\partial \psi(\omega)}{\partial n} \propto \frac{\omega_{Im}}{(\omega - \omega_{Re})^2 + \omega_{Im}^2}. \quad (17)$$

The sign of $\frac{\partial \psi(\omega)}{\partial n}$ is hence dictated by the position of the pole. For the regular dielectric slab or in normal phase of $\mathcal{PT}$ system, the poles remain in unphysical sheet and $\omega_{Im} > 0$. However, in anomalous phase of $\mathcal{PT}$ system, poles cross the real axis and move into physical sheet with $\omega_{Im} < 0$ and negative ψ near the pole. Therefore the sign of FR angle θ_1 changes as the pole moves across the real axis from unphysical to physical sheet, and remains negative as long as poles stay in physical sheet. This can be easily illustrated in Fig. 5. For the set of model parameters chosen in Fig. 5, one of the spectral singularities is located at $(\omega/c, \varphi_V) = (4.73, 0.277\pi)$. For φ_V value slightly below 0.277π, the pole is located in unphysical sheet, and θ_1 remains positive. As φ_V value is increased across 0.277π, the pole moves across the real axis into physical sheet, and hence θ_1 changes sign and becomes negative.

We remark that for a simple model, the pole indeed yields divergent spectral singularities when it lies on the real axis. As discussed in Ref. [43], in realistic systems, the divergence of spectral

singularities may be regularized by nonlinearities of systems. Similarly, the regularization of singularities in a realistic system can also be achieved by imperfection of $\mathcal{PT}$ systems with a slight imbalance between the gain and loss regions by adding an infinitesimal parameter to imaginary part of the right boundary complex potential.

At last we remark that the reversal of the sign of the Faraday rotation also occurs in some other special cases. For example, in Ref. [44], it was shown that near the plasmon resonance of Fe_2O_3 nanoparticles solution, the Faraday rotation exhibits both left and right rotations for fixed frequencies. The latter is due to the change in the sign of the Verdet constant, as a result of increasing the thickness of the gold shell with the addition of a gold solution. As also mentioned in Ref. [45], the Faraday rotation angle θ_1 can be increased and even changed its sign using metamaterials to adapt the optical properties of the host system. In addition, for the frequencies range where both complex permittivity ϵ and permeability μ have negative non-zero real parts and positive non-zero imaginary parts, the real part of n turns out to be negative, see, e.g. Ref. [46]. Hence, the angle θ_1, which is an odd function with respect to the refractive index n, will change the sign as well. As for θ_2, it is an even function of n and does not change sign when n is reversed [37]. The phase transition-like behavior in the change of sign of the Faraday rotation angle θ_1 in a $\mathcal{PT}$ system studied in this letter demonstrates a quite different mechanism from the cases mentioned above. The phase transition-like anomalous Faraday effect may be observed experimentally for the wider range of frequencies. Hence $\mathcal{PT}$-systems seem to be ideal candidates for constructing fast tunable polarization rotational ultrathin magneto-optical devices.

CRediT authorship contribution statement

Vladimir Gasparian: Writing – original draft. **Peng Guo:** Writing – review & editing. **Esther Jódar:** Writing – review & editing.

Declaration of competing interest

The authors declare that they have no known competing financial interests or personal relationships that could have appeared to influence the work reported in this paper.

Data availability

No data was used for the research described in the article.

Acknowledgements

References

[1] L.D. Landau, E.M. Lifshitz, Electrodynamics of Continuous Media, Pergamon, New York, 1984.

[2] M.S. Longair, High Energy Astrophysics, 3rd ed., Cambridge University Press, 2011.

[3] J.K. Furdyna, J. Appl. Phys. 64 (1988) R29, https://doi.org/10.1063/1.341700.

[4] U. Berger, in: R.A. Meyers (Ed.), Encyclopedia of Physical Science and Technology, third edition, Academic Press, New York, ISBN 978-0-12-227410-7, 2003, pp. 777–798, URL https://www.sciencedirect.com/science/article/pii/B0122274105004452.

[5] E.H. Turner, R.H. Stolen, Opt. Lett. 6 (1981) 322, http://opg.optica.org/ol/abstract.cfm?URI=ol-6-7-322.

[6] C.J. Firby, P. Chang, A.S. Helmy, A.Y. Elezzabi, J. Opt. Soc. Am. B 35 (2018) 1504, http://opg.optica.org/josab/abstract.cfm?URI=josab-35-7-1504.

[7] E. Garbusi, J.A. Ferrari, Opt. Laser Technol. (ISSN 0030-3992) 35 (2003) 319, URL https://www.sciencedirect.com/science/article/pii/S0030399203000100.

[8] N. Richard, A. Dereux, E. Bourillot, T. David, J.P. Goudonnet, F. Scheurer, E. Beaurepaire, J. Appl. Phys. 88 (2000) 2541, https://doi.org/10.1063/1.1288509.

[9] H. Uchida, Y. Mizutani, Y. Nakai, A.A. Fedyanin, M. Inoue, J. Phys. D, Appl. Phys. 44 (2011) 064014, https://doi.org/10.1088/0022-3727/44/6/064014.

[10] P. Andrei, I. Mayergoyz, J. Appl. Phys. 94 (2003) 7163, https://doi.org/10.1063/1.1625084.

[11] Z. Gevorkian, V. Gasparian, Phys. Rev. A 89 (2014) 023830, URL https://link.aps.org/doi/10.1103/PhysRevA.89.023830.

[12] R.M. Kaipurath, M. Pietrzyk, L. Caspani, T. Roger, M. Clerici, C. Rizza, A. Ciattoni, A. Di Falco, D. Faccio, Sci. Rep. 6 (2016) 27700, https://doi.org/10.1038/srep27700.

[13] J.B. Pendry, Phys. Rev. Lett. 85 (2000) 3966, URL https://link.aps.org/doi/10.1103/PhysRevLett.85.3966.

[14] S. Yang, P. Liu, M. Yang, Q. Wang, J. Song, L. Dong, Sci. Rep. 6 (2016) 21921, https://doi.org/10.1038/srep21921.

[15] V. Caligiuri, R. Dhama, K.V. Sreekanth, G. Strangi, A. De Luca, Sci. Rep. 6 (2016) 20002, https://doi.org/10.1038/srep20002.

[16] T. Cao, C. Wei, R.E. Simpson, L. Zhang, M.J. Cryan, Opt. Mater. Express 3 (2013) 1101, URL http://opg.optica.org/ome/abstract.cfm?URI=ome-3-8-1101.

[17] C.M. Bender, P.E. Dorey, C. Dunning, A. Fring, D.W. Hook, H.F. Jones, S. Kuzhel, G. Lévai, R. Tateo, PT Symmetry, World Scientific (Europe), 2019, URL https://www.worldscientific.com/doi/pdf/10.1142/q0178.

[18] C.M. Bender, Contemp. Phys. 46 (2005) 277, https://doi.org/10.1080/00107500072632.

[19] V.V. Konotop, J. Yang, D.A. Zezyulin, Rev. Mod. Phys. 88 (2016) 035002, URL https://link.aps.org/doi/10.1103/RevModPhys.88.035002.

[20] A. Mostafazadeh, Int. J. Geom. Methods Mod. Phys. 07 (2010) 1191, https://doi.org/10.1142/S0219887810004816.

[21] A. Mostafazadeh, Pramana 73 (2009) 269, https://doi.org/10.1007/s12043-009-0118-4.

[22] R. El-Ganainy, K.G. Makris, M. Khajavikhan, Z.H. Musslimani, S. Rotter, D.N. Christodoulides, Nat. Phys. 14 (2018) 11, https://doi.org/10.1038/nphys4323.

[23] K.G. Makris, R. El-Ganainy, D.N. Christodoulides, Z.H. Musslimani, Phys. Rev. Lett. 100 (2008) 103904, URL https://link.aps.org/doi/10.1103/PhysRevLett.100.103904.

[24] Z.H. Musslimani, K.G. Makris, R. El-Ganainy, D.N. Christodoulides, Phys. Rev. Lett. 100 (2008) 030402, URL https://link.aps.org/doi/10.1103/PhysRevLett.100.030402.

[25] B. Bagchi, S. Mallik, H. Bíla, V. Jakubský, M. Znojil, C. Quesne, Int. J. Mod. Phys. A 21 (2006) 2173, https://doi.org/10.1142/S0217751X0602951X.

[26] Y.N. Joglekar, B. Bagchi, J. Phys. A, Math. Theor. 45 (2012) 402001, https://doi.org/10.1088/1751-8113/45/40/402001.

[27] A. Mostafazadeh, Phys. Rev. Lett. 102 (2009) 220402, URL https://link.aps.org/doi/10.1103/PhysRevLett.102.220402.

[28] Z. Ahmed, J. Phys. A, Math. Theor. 42 (2009) 472005, https://doi.org/10.1088/1751-8113/42/47/472005.

[29] S. Longhi, Phys. Rev. B 80 (2009) 165125, URL https://link.aps.org/doi/10.1103/PhysRevB.80.165125.

[30] L. Ge, Y.D. Chong, A.D. Stone, Phys. Rev. A 85 (2012) 023802, URL https://link.aps.org/doi/10.1103/PhysRevA.85.023802.

[31] C. Hang, G. Huang, V.V. Konotop, Phys. Rev. Lett. 110 (2013) 083604, URL https://link.aps.org/doi/10.1103/PhysRevLett.110.083604.

[32] C. Hang, D.A. Zezyulin, G. Huang, V.V. Konotop, B.A. Malomed, Opt. Lett. 39 (2014) 5387, URL http://opg.optica.org/ol/abstract.cfm?URI=ol-39-18-5387.

[33] H. Alaeian, J.A. Dionne, Phys. Rev. A 89 (2014) 033829, URL https://link.aps.org/doi/10.1103/PhysRevA.89.033829.

[34] H. Alaeian, J.A. Dionne, Phys. Rev. B 89 (2014) 075136, URL https://link.aps.org/doi/10.1103/PhysRevB.89.075136.

[35] X. Zhu, H. Ramezani, C. Shi, J. Zhu, X. Zhang, Phys. Rev. X 4 (2014) 031042, URL https://link.aps.org/doi/10.1103/PhysRevX.4.031042.

[36] V. Gasparian, M. Ortuño, J. Ruiz, E. Cuevas, Phys. Rev. Lett. 75 (1995) 2312, URL https://link.aps.org/doi/10.1103/PhysRevLett.75.2312.

[37] J. Lofy, V. Gasparian, Z. Gevorkian, E. Jódar, Rev. Adv. Mater. Sci. 59 (2020) 243, https://doi.org/10.1515/rams-2020-0032.

[38] P. Guo, V. Gasparian, Phys. Rev. Research 4 (2022) 023083, URL https://link.aps.org/doi/10.1103/PhysRevResearch.4.023083.

[39] P. Carpena, V. Gasparian, M. Ortuño, Z. Phys. B, Condens. Matter 102 (1997) 425, https://doi.org/10.1007/s002570050307.

[40] V. Gasparian, T. Christen, M. Büttiker, Phys. Rev. A 54 (1996) 4022, URL https://link.aps.org/doi/10.1103/PhysRevA.54.4022.

[41] L. Ge, K.G. Makris, D.N. Christodoulides, L. Feng, Phys. Rev. A 92 (2015) 062135, URL https://link.aps.org/doi/10.1103/PhysRevA.92.062135.

[42] P. Guo, V. Gasparian, E. Jódar, C. Wisehart, arXiv:2208.13543, 2022.

[43] X. Liu, S.D. Gupta, G.S. Agarwal, Phys. Rev. A 89 (2014) 013824, URL https://link.aps.org/doi/10.1103/PhysRevA.89.013824.

[44] R.K. Dani, H. Wang, S.H. Bossmann, G. Wysin, V. Chikan, J. Chem. Phys. 135 (2011) 224502, https://doi.org/10.1063/1.3665138.

[45] M. Sadatgol, M. Rahman, E. Forati, M. Levy, D.Ö. Güney, J. Appl. Phys. 119 (2016) 103105, https://doi.org/10.1063/1.4943651.

[46] J. Pendry, Contemp. Phys. 45 (2004) 191, https://doi.org/10.1080/00107510410001667434.